Penerbit Akademia Baru

CFD Letters

Journal homepage: www.akademiabaru.com/cfdl.html
ISSN: 2180-1363

Heat Transfer Across Tube Banks With a Passive Control Vortex Generator in Steady One-Directional and Oscillatory Flows.

Open Access

Chou Aw Lin[1], Fatimah Al-Zahrah Mohd Sa'at[1,2,3*], Fadhilah Shikh Anuar[2,4], Muhammad Firdaus Sukri[1,2], Mohd Zaid Akop[1,2], Zainuddin Abdul Manan[5]

[1] Fakulti Kejuruteraan Mekanikal, Universiti Teknikal Malaysia Melaka, Hang Tuah Jaya, 76100 Durian Tunggal, Melaka, Malaysia
[2] Centre for Advanced Research on Energy (CARe), Universiti Teknikal Malaysia Melaka, Hang Tuah Jaya, 76100 Durian Tunggal, Melaka, Malaysia
[3] Center of Excellence Geopolymer and Green Technology, Universiti Malaysia Perlis, 01000 Kangar, Perlis, Malaysia
[4] Fakulti Teknologi Kejuruteraan Mekanikal dan Pembuatan, Hang Tuah Jaya, 76100 Durian Tunggal, Melaka, Malaysia
[5] Process System Engineering Centre (PROSPECT), Faculty of Chemical and Natural Resources Engineering, Universiti Teknologi Malaysia, 81310 Skudai, Johor, Malaysia

ARTICLE INFO

Article history:
Received 22 November 2020
Received in revised form 16 January 2021
Accepted 23 January 2021
Available online 30 January 2021

ABSTRACT

Fluid can flow in one-directional (normal flow) or oscillatory conditions. Fluid flow in some energy system involved oscillatory flow condition. The use of vortex generator has been proven to improve heat transfer in the case of one-directional flow but the impact of vortex generator in oscillatory flow condition is yet unknown. This study focusses on the heat transfer performance across a heated tube banks using a Computational Fluid Dynamics (CFD) model. Two flow conditions were modelled: steady one-directional and oscillatory flow conditions. Two-dimensional CFD models of steady flow and oscillatory flow were solved using the SST k-ω turbulence model for two different cases of heated tube banks with and without the vortex generators. The heat transfer performance for both flow conditions were analysed by considering a heat transfer parameter known as Colburn-j factor. Results showed that the use of a vortex generator increased the heat transfer enhancement, regardless of the flow conditions. However, it is also noted that the heat transfer behaviour in a steady flow and an oscillatory flow is not the same, especially with the appearance of secondary flows in the system. The difference is discussed with respect to dimensionless quantity of Colburn j-factor, the non-dimensionless quantity, and the amplitude of temperature field. The result indicates that the heat equation in the steady flow condition is not very suitable to be directly used in oscillatory flow conditions. Appropriate heat equation needs to be properly addressed for situations that involve oscillatory flow motion.

Keywords:
Vortex generator; heat exchanger; steady flow; oscillatory flow; CFD

* *Corresponding author.*
E-mail address: fatimah@utem.edu.my (Fatimah Al-Zahrah Mohd Sa'at)

https://doi.org/10.37934/cfdl.13.1.118

1. Introduction

Tube banks heat exchanger is popular and it is an unmixed flow arrangement where the process of heat exchange involves two fluids at different temperatures; the first fluid flows in the tubes while the second fluid flows outside of the tubes in the shell. The performance of a heat exchanger can be improved using passive control techniques, and a vortex generator is one of the promising ways to augment the heat transfer, subjected to its arrangement. For example, transverse vortices are two-dimensional flow which the axes are normal to the direction of fluid flow. Transverse vortices increase the intensity of turbulence by destabilizing flow while longitudinal vortices, which is three-dimensional flow with axes parallel to the flow direction diminish poor heat transfer region [1]. It was found that the longitudinal vortices have a better heat transfer rate over transverse vortices, as more heat transfer mechanism can be considered and the effect at the affected region also last longer as it continues further down the flow direction. Furthermore, the heat transfer rate of longitudinal vortices can be further improved by introducing delta winglets on fin-and-oval tube heat exchanger [2,3].

Awais and Bhuiyan [3] had tested several cases study with different parameters including number of rows, attack angles, tube configurations, attack angle, vortex generator configuration and tube shapes. The best configuration is determined based on heat transfer enhancement with the lowest pressure drop penalty. From the research and study of Awais and Bhuiyan [3] and Torri, Kwak and Nishino [4], it is showed that higher heat transfer rate is incorporated with higher ratio of Colburn j-factor and ratio of friction of flow which were donated as j/j_o and f/f_o, respectively. This is because with higher j/j_o value, it is shown that the local velocity of the fluid relatively increases, thus increasing turbulent intensity of the fluid. Through the research done by Torii *et al.,* [4], they found out that the application of vortex generator enhances the heat transfer performance while decreasing the pressure drop. They also mentioned that delta winglet pair vortex generator enhances the heat transfer performance in low Reynolds number fluid flow. Salvanio *et al.,* [5] introduced the objective function, *JF*, which consider the Colburn-j factor and friction factor. They found out that the vortices effect is stronger for staggered tubes, and the heat transfer enhancement are optimum at a fin-pitch of 0.6. Li *et al.,* [6] did an experiment to study the heat transfer enhancement of a pin-fin heat sink by using vortex generator. The heat transfer enhancement is indicated through the thermal resistance that considers the heat sink temperature, ambient temperature, and the heating power. In the study done by Zhai and Islam *et al.,* [7], parameter of thermal performance enhancement (TEF) was used to measure the heat transfer performance in their study. The heat transfer performance in their study is tested with the parameter of Nusselt number, Nu, and friction factor, *f*, considering Nu as the heat performance indicator and *f* as the penalty of the performance. Song *et al.,* [8] did an experimental study on application of curved delta winglet vortex generators in heat exchangers. They used a ratio of Colburn-j factor to friction ratio to indicate the heat transfer performance. They found out that curved vortex generators helped to maintain the flow separation and further reduced the wake region. In their experiment, it is noted that the fin-pitch has a larger effect on the friction ratio compared to the Colburn-j ratio. Zdanski *et al.,* [9] did an experiment on evaluating the best configuration for inline tubes where the heat transfer performance is analysed using Nusselt Number with a new correlation of delta winglet pitch and cylindrical heaters diameter. It is found that the heat transfer is optimum when the ratio of vortex generator and tube bank distance to cylindrical heaters diameter is 1.94, with an incident angle of 40°.

Basically, the vortex generators generate vortices in fluid flow by inducing secondary swirling flow: vortices around the vortex generators. These vortices push the fluid flow through the poor heat transfer region behind the tubes. Fluids at this wake region is pushed out to the mainstream region.

This highly reduce the wake region behind the tubes, and thus increasing heat transfer in the heat exchanger. The vortex generator can be mounted on the tube banks surface to control boundary layer separation and improving the heat transfer process effectively. Vortices may decrease the boundary layer thickness and further increase the intensity of the secondary flow in the heat exchanger.

One will intuitively assume that the use of a vortex generator in two different flow conditions, (steady one directional and oscillatory flows) may result in different flow behaviors and heat transfer rates. However, for the oscillatory flow motion, there is no definite way in heat transfer calculation for an oscillatory flow [10]. Experimental study showed that heat transfer coefficient of oscillatory flow of thermoacoustics is also depending on the cyclic nature of the oscillatory flow. Their study on heat transfer was done by using the calorimetric method by measuring the heat transfer rate at the higher temperature side of the heat exchanger, while the low temperature side rejects heat to the surrounding. The study suggested the use of the heat transfer rate and dimensionless heat transfer coefficient such as the Colburn-j factor that considers the relations between heat transfer coefficient, fin spacing, thermal conductivity, acoustic Reynolds number and Prandtl number. The use of root mean square Reynolds number (RMS-Re) to obtain the acoustic Reynolds Number and time-averaged steady-flow equivalent (TASFE) model was later suggested for a correct calculation of Nusselt number for thermal performance calculation [11]. Jaworski and Piccolo [12] also reported numerical models of oscillatory flow that was validated by experimental results. Nusselt number was used as an indication of thermal performance where the data computed are all time-averaged quantities. Their numerical approach predicts the heat transfer coefficient at a 41% confidence level. Illori *et al.,* [13] did an experimental and numerical studies of the thermal performance of a heat exchanger in a thermoacoustics with oscillatory flow condition. They suggested a modification in the experimental setup by introducing heat exchanger edge shapes. The study was done by integrating the experiment al work with the Computational Fluid Dynamics Model. The parameters were then compared between the experimental and numerical approaches. The experimental and numerical approaches showed a good agreement. It was reported that the heat transfer performance can be improved by using heat exchanger edge shapes while minimising the pressure drop. Anas and Xiaoqing [14] introduced a new approach of artificial neural network (ANN) model to predict the oscillatory heat transfer coefficient for thermoacoustic heat exchanger. The developed ANN model was a model driven by a pure data. The model consists of interconnecting nodes knowingly artificial neurons that predicts the heat transfer coefficient through numerous computations of existing input and output data. Elaziz *et al.,* [15] did a numerical study using adaptive neuro-fuzzy inference system (ANFIS) to predict the oscillatory heat transfer coefficient. The model used in their study is an ANN-based system consisting a combination of ANFIS and Crow Search Algorithm (CSA). Their study similarly consists of two parts which first analyse the given input and output data, then it is further used to analyse and test other input data. They found out that this system has a better prediction over the conventional ANFIS system and ANFIS base genetic algorithm. Chen *et al.,* [16] did a large eddy simulation model to evaluate the performance of a thermoacoustic engine. The thermoacoustic engine is evaluated from four aspects which is the dynamic characteristics of the engine during initial start-up process, acoustic behavior of the engine at steady state, hydrodynamic performance of the engine, and heat transfer characteristics inside the engine. The heat transfer characteristics is analysed using mean temperature and transversal heat fluxes. They showed that large eddy simulation effectively analyzed the standing-wave thermoacoustics engine with the supports of high-performance computing and high fidelity three-dimensional (3D) simulation. Feng *et al.,* [17] studied the performance of a jet pump inside a thermoacoustic engine. They used the overall resistance to evaluate the performance of the thermoacoustic engine. However, they found that the jet pump only

enhances thermal performance at a small taper angle that is smaller than 9°. Rahpeima and Ebrahimi [18] and Yahya *et al.,* [19] did a study on thermoacoustic refrigerators. They proposed the use of coefficient of performance (COP) to evaluate the performance of the thermoacoustic refrigerators. The study of Rahpeima and Ebrahimi [18] focused on the stack geometrical while Yahya *et al.,* [19] studied the stack materials in thermoacoustics. Rahpeima and Ebrahimi [18] concluded that the stack thickness should be as small as possible and the distance between stacks should be around 2 to 4 times of the thermal penetration depth so that good heat transfer performance could be achieved in the system. Whilst Yahya *et al.,* [19] found that steel wool stacks provided the maximum cooling power for their investigated system.

For the steady flow, the heat transfer can be represented by the effect of Reynolds number on friction ratio or Colburn ratio and the pressure drop on different Reynolds [20,21]. In addition, visualization on several parameters such as velocity, pressure and temperature distribution could also be analysed to understand the changes in heat transfer process [3]. The use of vortex generator has been shown to be useful for flow across tube banks in one-directional flow condition. However, the use of vortex generator for heat exchanger utilized in thermoacoustic environment have not yet been investigated. There are plenty of rooms to be investigated when it comes to heat transfer of oscillatory flow in thermoacoustics [22]. It is interesting to investigate the possibility of heat enhancement for thermoacoustic environment should the vortex generator be applied to the heat exchanger in the system. The flow in thermoacoustic environment is oscillatory in nature and heat exchanger is one of the most important part of the system. In this study, the effect of the vortex generator towards the heat transfer performance across tube banks in steady one-directional and oscillatory flows are studied and analysed.

2. Methodology

The study is done by analysing the fluid flow in heat exchanger with the presence of vortex generator through numerical simulation. ANSYS Fluent is used to simulate the fluid flow. The numerical simulation consists of pre-processing, solving, and post-processing steps. Pre-processing step consists of geometry modelling as shown in Figures 1 and 2. Sets of computational mesh are then constructed, and the mesh quality of the computational domain is as shown in Figure 2(b). The tubes are arranged in staggered manner with 165° angle of attack (vortex generator) and the tube is circular in shape.

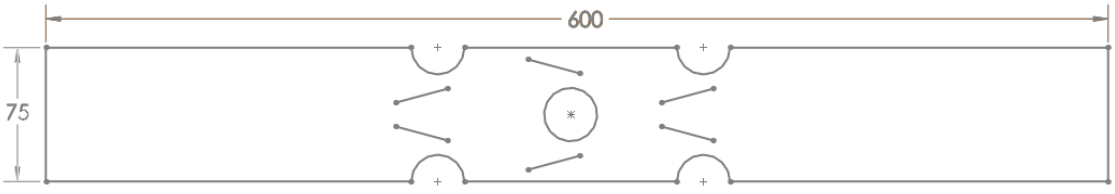

Fig. 1. Dimension of the computational domain in unit millimetre

A heat exchanger tube banks geometry as drawn in Figure 1 and Figure 2 was set with two different conditions: the steady one-directional flow condition and the oscillatory flow condition. For steady flow model, the steady boundary conditions are set at the inlet and outlet boundaries of the computational domain. The top and bottom boundaries of the computational domain were set as symmetrical wall while the walls of the circular tube and the vortex generator are set as smooth walls with no-slip boundary condition. The tube temperature was set to be at 350 K. The inlet boundary of the model was set with velocity values ranging from 0.49 m/s to 2.83 m/s. The inlet temperature was

312 K. The outlet boundary condition was set as an outflow boundary conditions where zero diffusion flux were assigned for all flow variables that cross this boundary. This satisfies the Neumann Boundary Condition where conditions at the wall between the cells on the left and right sides adjacent to the boundary are the same hence the gradient is zero. This represents no immediate change of flow at the boundary when the fluid is about to leave the domain. The models were solved as two-dimensional problem.

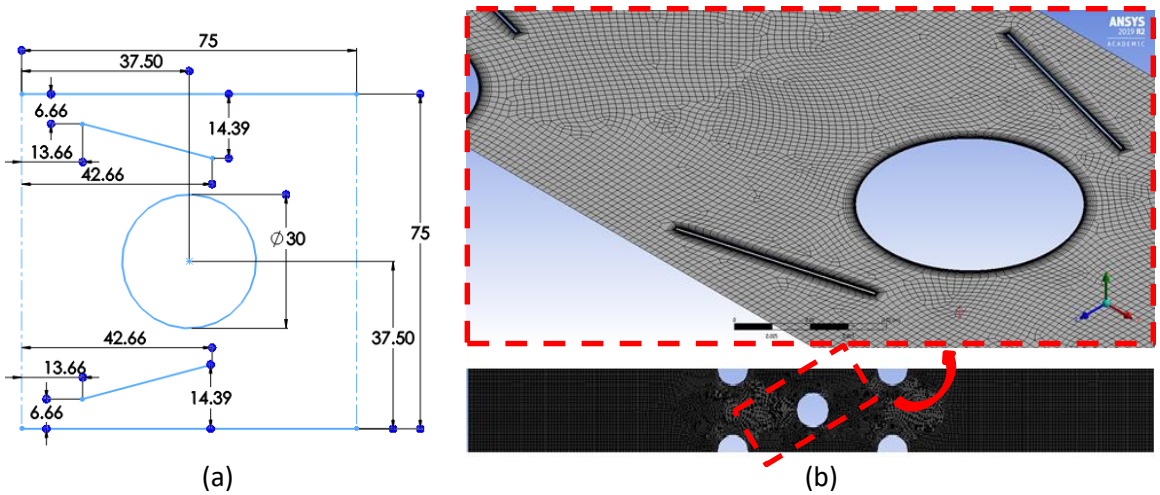

Fig. 2. (a) Dimension (in unit millimetre) for the geometry of a single tube and a pair of vortex generator and (b) the mesh of the computational domain with enlarged view around the area of tube and vortex generator

In oscillatory flow model, the boundary conditions at the tube walls and the vortex generator remains the same but the boundary conditions at the inlet and outlet were set to follow the oscillatory nature of flow. The oscillatory flow condition was modelled based on the oscillatory flow that may be found in thermoacoustic environment. Oscillating pressure at the inlet and the outlet was set with oscillating mass flux. The equations for inlet and outlet conditions are shown in Eq. (1) and Eq. (2). Both assignments of inlet and outlet conditions were done using a user defined function (UDF). The values of all the parameters defined in Eq. (1) and Eq. (2) are listed in Table 1. The oscillating flow condition is represented by a term known as a drive ratio, DR, which is defined as the ratio between the pressure at the location of pressure antinode, Pa, and the mean pressure of the flow, P_m. This is as shown in Eq. (3). In general, the drive ratio also represents the amplitude of flow. As the drive ratio increases, the flow amplitude also increases. Oscillatory flow travels following the harmonic motion of the wave. For this study, the oscillatory flow condition was modelled for a flow frequency of 14.2 Hz where the corresponding wave number, k, and the wavelength, λ, are as described in Eq. (4), and Eq. (5) (where t is time), respectively. The frequency was chosen based on works reported by Mohd Saat and Johari [23].

$$P = P_a \cos(kx_1) \cos(2\pi f t) \tag{1}$$

$$m' = \frac{P_a}{c} \sin(kx_2) \cos(2\pi f t + \theta) \tag{2}$$

$$DR = \frac{P_a}{P_m} \tag{3}$$

$$k = \frac{2\pi f t}{c} \tag{4}$$

$$\lambda = \frac{c}{f} \quad (5)$$

Table 1
Operating conditions in oscillating flow

Parameters	Symbol	Value
Mean Pressure	P_m	100000 Pa
Frequency	f	14.2 Hz
phase shift between velocity and pressure	ϑ	1.57 rad
speed of sound	c	346 m/s

The walls were all set with material properties of Aluminium while air was used as a working fluid in this study. The air was treated as an ideal gas. The thermal conductivity of air was modelled as temperature dependence using the piecewise-polynomial function with eight coefficients. The eight coefficients are 0.023635, 7.56264e^{-05}, -2.51537e^{-08}, 4.18521e^{-12}, 1.05973e^{-15}, -1.12111e^{-18}, 5.47329e^{-22}, and -9.94835e^{-26}, respectively. The governing equations used in this study are the energy equation, the mass conservation equation, and the momentum conservation equation. As the computational domain consists of staggered tubes and vortex generators, the momentum of flow was modelled using the SST (Shear Stress Transport) *k-ω* turbulence so that better capture of fluid dynamics within the viscid and inviscid regions can be obtained [2]. The summary of material properties is given in Table 2.

Table 2
Properties of the air and materials used

Material	Density, ρ (kg/m^3)	Specific heat, C_p (J/kg.K)	Thermal conductivity, κ (W/m.K)	Kinematic viscosity, ν (kg/m.s)	Diffusivity, α (m^2/s)
Air	Ideal air	1006.43	Piecewise polynomial	1.568×10^{-5}	22.07×10^{-6}
Aluminum	2719	871	202.4	-	-

Grid Independency test was done to check the sensitivity of the solution to the change of mesh size. Mesh for the computational domain were set from 100000 up to 250000 nodes and the velocity results from the models with different mesh sizes were compared and shown in Table 3. Mesh numbers of 250000 was found sufficient to provide solution that is grid independent with sensitivity of around 1.3% between the tested mesh numbers. This leads to meshes with an average size of 0.71 mm. Small size meshes (with minimum size of 0.09 mm) were applied near the wall to capture the boundary layer changes of flow within this region. Further increase in mesh numbers will lead to too long a computational time especially for transient case of oscillatory flow. Hence the model is solved with computational domain with total mesh of 250000 and the mesh is as shown in Figure 2 (b).

Table 3
Maximum velocity tabulated against different nodes

Nodes	100000	150000	200000	250000
V_{max} (m/s)	3.18609	3.07131	2.94916	2.91022

The models were also verified and validated by comparing the results with the published data and theoretical calculation, whenever possible. The theoretical values of the amplitudes of mass flux, m'_1, and velocity, *V*, of the oscillatory flow can be calculated using Eq. (6) and Eq. (7) where x_2 is the location from the pressure antinode (the location with maximum pressure amplitude).

$$m'_1 = \frac{P_a}{c}\sin(kx_2) \quad (6)$$

$$V = \frac{m\prime}{\rho} \tag{7}$$

3. Model Validation and Verification

The steady model was validated with the results of Awais and Bhuiyan [3]. Comparison was done based on the Colburn j-factor ratio between the current CFD results and the experimental and numerical results of Awais and Bhuiyan [3]. The result is as shown in Figure 3. It is noteworthy that, for the purpose of model validation, the CFD models were solved using the same conditions as reported by Awais and Bhuiyan [3]. Colburn-j ratio, j/j_0, is obtained by dividing the Colburn j value to the reference value of j_0. The reference value of j_0 was calculated using the same calculation on a model with the same boundary conditions and setting but without the presence of vortex generators.

The Colburn-j number is calculated using Eq. (8), where the Prandtl number, Pr, can be calculated using Eq. (11). The Nusselt number, Nu, and the heat transfer coefficient, h, are obtained following Eq. (9) and Eq. (10). The parameter used in the steady flow condition is as listed in Table 4.

$$j = \frac{Nu}{Re(Pr^{1/3})} \tag{8}$$

$$Nu = \frac{h2H}{\kappa} \tag{9}$$

$$h = \frac{q'}{T_{wall} - T_f} \tag{10}$$

$$Pr = \frac{v}{\alpha} \tag{11}$$

Table 4
Operating conditions in steady flow model

Parameters	Symbol	Value
Thermal conductivity	κ	0.0242 W/m.K
Fin Spacing	H	0.0056 m
Tube wall temperature	T_{wall}	350 K
speed of sound	c	346 m/s
Kinematic viscosity	v	1.568×10^{-05} kg/ms
Diffusivity	α	22.07×10^{-06} m^2/s

The results of present study are shown in Figure 3, and the computed values are shown to fall within the range of values reported by Awais and Bhuiyan [3]. It is interesting to note that our CFD models provide results that are closer to the reported experimental data compared to their own numerical results especially at high ranges of Reynolds numbers. This was probably due to the improved numerical model in the present study which includes larger computational domain compared to theirs. This indicates that simplification of computational domain does have an impact on the numerical results. By considering domain to cover more tubes within the direction of flow, the numerical results become closer to experimental values.

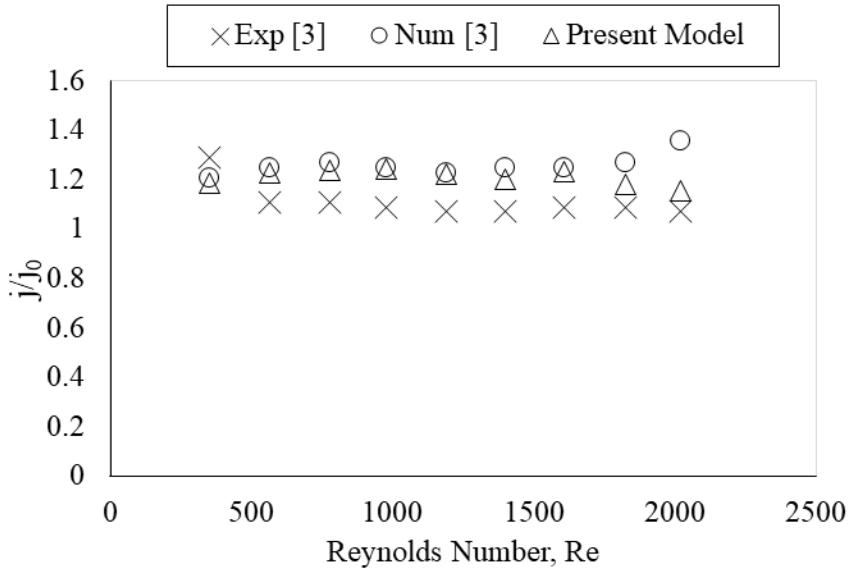

Fig. 3. Comparison of results between published experimental and numerical values with the values of present CFD study

For oscillatory flow conditions, the model was verified by comparing velocity amplitude data at a specific point of 0.2 m from the mass flux inlet boundary and 0.325 m from the bottom symmetrical boundary for three different flow conditions. The results are as shown in Figure 4. The theoretical values are obtained using Eq. (6) and Eq. (7).

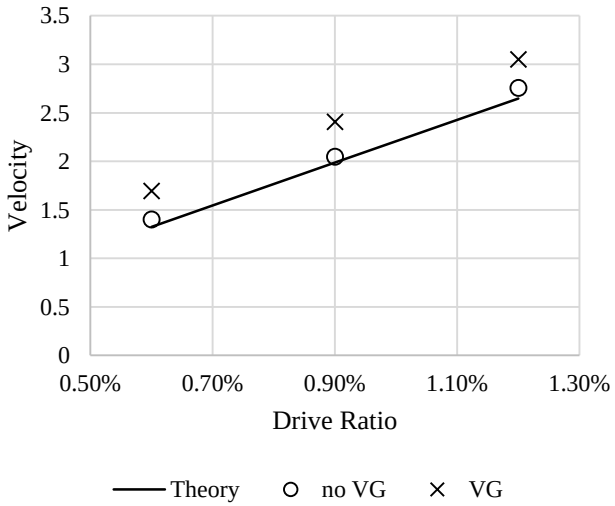

Fig. 4. Comparison of velocity amplitude for cases with and without vortex generator (VG) at three different drive ratios with the theoretical value for oscillatory flow condition

The computed theoretical value is then compared with the velocity value obtained from ANSYS at the same specific location. The models were solved for two cases: with the presence of vortex generator and without the presence of the vortex generator. It is shown in Figure 4 that the velocity amplitude for cases without the presence of vortex generator is slightly higher than the theoretical value. This slight difference is probably happening due to the presence of the tube inside the flow

domain. The theoretical value of velocity for the oscillatory flow condition does not consider the changes of flow due to the presence of the tubes. When there is tube in the flow, there will be slight differences between the theoretical value and the numerical calculation. The deviations of velocity are small, within 3. 0 % to 5.7 % of increment. For cases where vortex generators are adjunct to the same models, the velocity amplitude becomes larger than the no-vortex generator cases. Clearly, the presence of vortex generator increases the velocity amplitude within the area. The velocity increments are recorded to be in between 15.14% at low drive ratio and 27.92% at high drive ratio. Similar increment trends between numerical and theoretical values mean that the oscillatory flows are correctly modelled by the CFD models. The small differences are probably due to variation of flow structures across the tube banks and the vortex generator in these two different methods.

4. Results and Discussions

Heat transfer between solid surface and fluid adjacent to it often depends on the fluid dynamics of the flow. Hence, the results from both the steady one-directional flow and the oscillatory flow models are shown based on the fluid dynamics representation of flow (i.e. velocity and vorticity) as well as the heat transfer parameters such as temperature and the Colburn j-factor.

4.1 Steady Flow

All temperature contour, velocity vector, and vorticity contour plots are done on the surface as shown in Figure 5. Figure 6 illustrates the contour plots for temperature, velocity, and vorticity from CFD model of steady one-directional flow at inlet velocity of 2.55 m/s with and without the presence of vortex generator. It shows that the fluid can be pushed through the leading edge of the vortex generator, resulting to fluid acceleration in between the vortex generator as shown in velocity plot in Figure 6(a). The vortex generator also induces secondary flows which generate longitudinal vortices in between the vortex generator and also behind the tubes as illustrated in the velocity vector in Figure 6(a). The fluid is forced to flow through the wake region behind the tube, reducing the original size of wake region in the case of no VG embedded in tube banks. This can be seen through the comparison between temperature contour of Figure 6 that shows the size of poor heat transfer wake region behind the tube is significantly reduced when vortex generator is used. The heat transfer was calculated to be increased by 15.56% in the presence of vortex generator.

Fig. 5. Post-CFD contour surface

The vorticity contour in Figure 6 shows the comparison of vorticity contour between cases with and without vortex generator. In the absence of vortex generator (right plot), a pair of an elongated vortex can be seen attached to the tubes. However, this elongated vortex appears weak with the presence of vortex generator. Clearly, the addition of vortex generator causes more intense vortex of small sizes. These intense small sizes vortices indicate an intense rotational of flow that happens within the area of the tube banks. The rotationality of flow can be seen in the vorticity contour of Figure 6. The travels of high intensity vortices of small sizes break the wake at the back of the tube structure (downstream) and this improves heat transfer between the tube and the fluids.

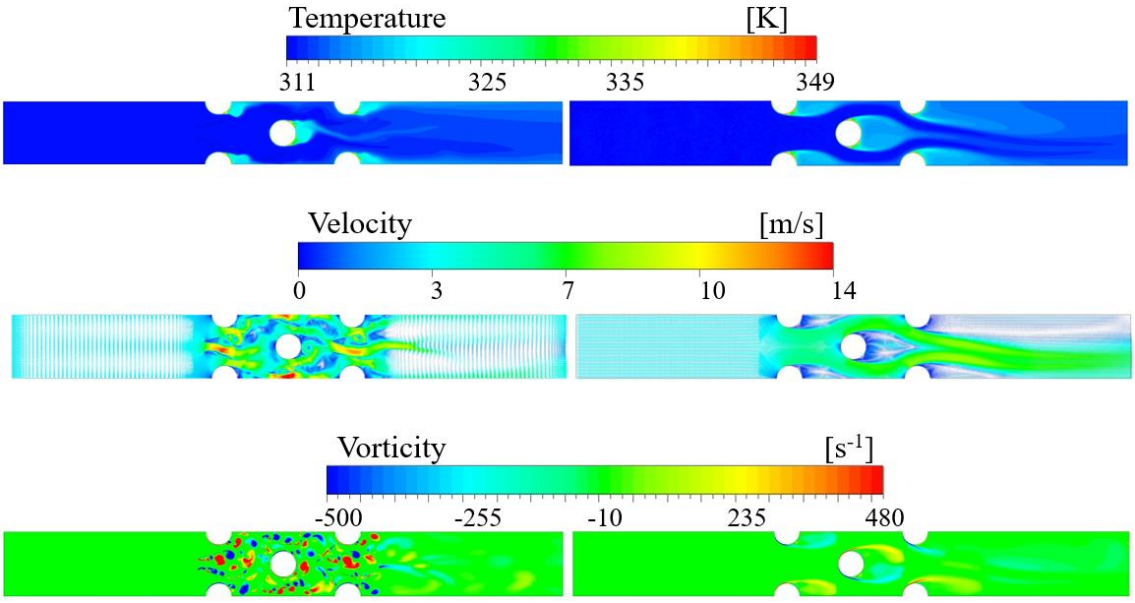

(a) With vortex generator (b) Without vortex generator

Fig. 6. Visualization of temperature, velocity, and vorticity for with VG and without VG

Figure 7 illustrates the temperature, velocity, and vorticity results within the area of the tubes for three different velocity values (1.37 m/s – 2.55 m/s) in steady flow condition for cases with the presence of vortex generator.

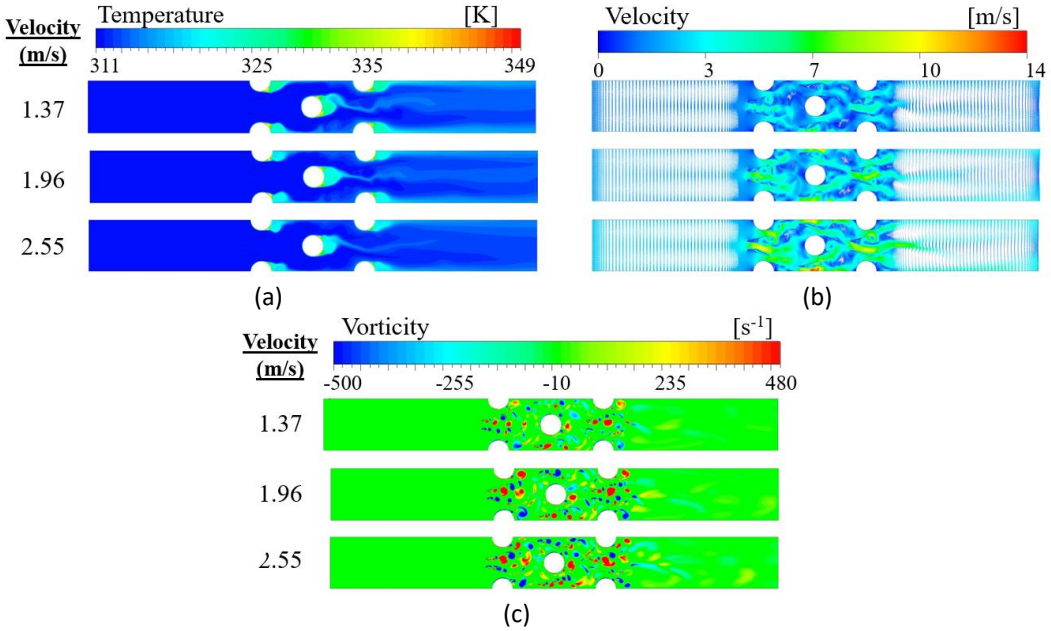

Fig. 7. Visualization of temperature contour, velocity vector, and vortex contour plot for 1.37 m/s,1.96 m/s, and 2.55 m/s

Naturally when velocity increases the vorticity also increases. The increase of vorticity is due to higher velocity creating vortices of higher intensity. However, with increasing velocity, the temperature distribution at downstream location after the tubes is lower, which indicates that lower amount of heat is transferred in between the heated tubes and fluids. This can be seen by looking closely at the colour of temperature contour in the downstream location to the right side of the tube walls. When fluid flows in high velocity, momentum by the high velocity fluid separates the fluid more

easily, creating a more significant wake region. As a result, the heat is not able to be brought out effectively by the cold fluid before leaving the heat exchanger.

4.2 Oscillatory Flow

Oscillatory flow condition is a condition of fluid flow where fluid oscillates across the field in a cyclic manner. In one flow cycle, fluid flows forward during the first half of the cycle and reverses during the second half of the cycle. This kind of flow can be found in energy system such as thermoacoustics. The temperature contour, vorticity contour, and velocity vector plot for oscillatory flow case at a drive ratio of 1.2% with and without the presence of vortex generator throughout the whole periodic of one flow cycle is shown in Figure 8, 9 and 10, respectively. The results are for 10 different stages within a flow cycle. The first five plots on top of the figure represents the first half of the cycle (i.e. fluid flows to the right) while the remaining five plots at the bottom are for the second half of the cycle (fluid reverses). The results are shown for cases with vortex generator (left) and without the vortex generator (right). It can be seen that the heat effects are following the fluid that oscillates forth and back across the tube banks.

In Figure 8, the heat distribution seems to be more evenly distributed throughout the system when vortex generator is presence. The heat is pushed further away from the tube. For the oscillatory flow without the presence of the vortex generator, the heat remains within the area of the tubes. Heat transfer is therefore more efficient with the presence of vortex generator since the heat from the tube is removed effectively.

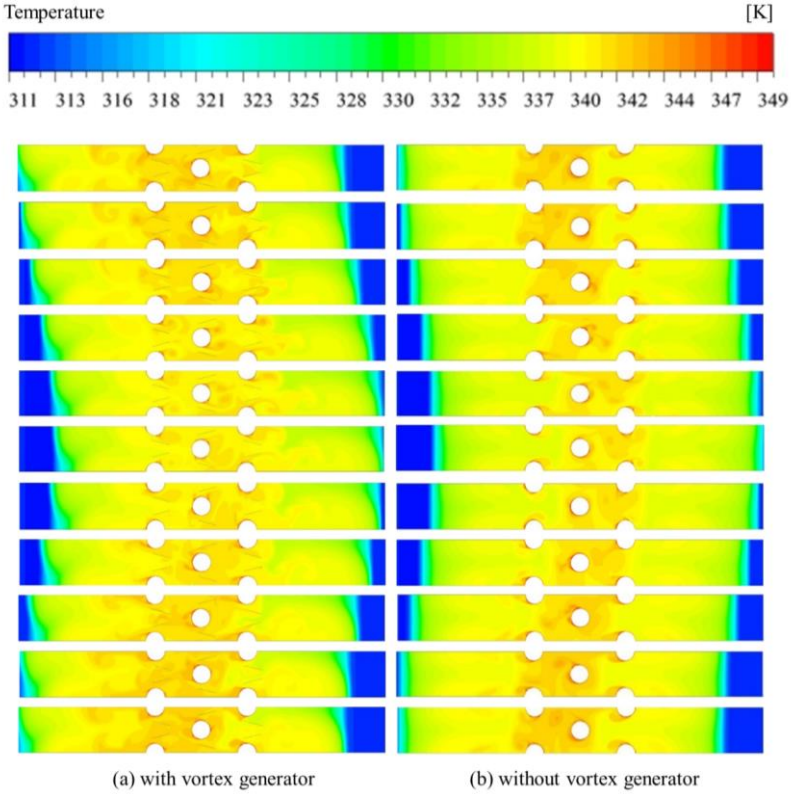

Fig. 8. Temperature contour within one flow cycle for oscillatory flow at a drive ratio of 1.2%

Figure 9 shows a significant increase of vortices are seen in the flow area near the tube banks when vortex generator is applied. The vortices are created mainly behind the vortex generator and

tubes following the direction of the flow. These vortices will oscillate back and forth following the cyclic nature of the flow and this cyclic flow influences the heat transfer performance. This happens repeatedly over the entire period of the oscillatory flow condition.

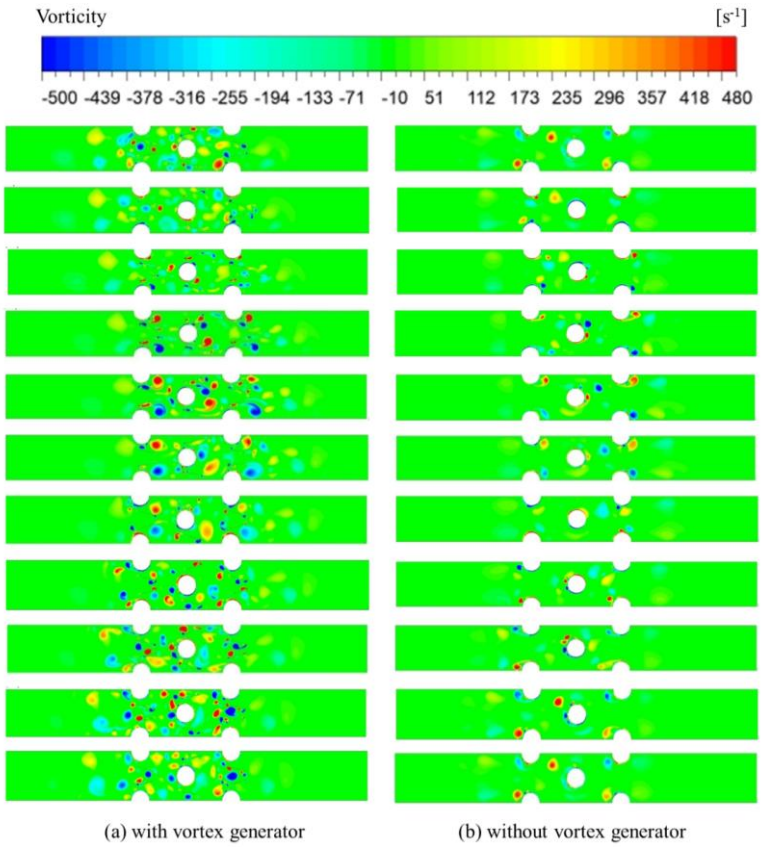

Fig. 9. Vorticity contour for one flow cycle for oscillatory flow at a drive ratio of 1.2%

Figure 10 shows that the presence of vortex generator creates a secondary flow between the tube and vortex generator and also between the gap of two vortex generators. The secondary flow in this case is referred to as the separated flow where portion of fluid is separated from the mainstream and appears as a part of fluid with its velocity slightly different than that of the mainstream. The secondary flow as seen in Figure 10 causes fluid flow to accelerate and as a results velocity increases throughout the system as compared to the case with an absence of the vortex generator. The changes of direction of velocity of flow can be seen throughout the ten stages of a flow cycle. During the first half of the cycle, fluid flows forward to the right direction. At the second half of the cycle, fluid reverses to the left side.

Figure 11 shows the contour and vector plots for oscillatory flow cases with different drive ratios. In general, the behaviour of velocity and vorticity are almost similar to the behaviour of flow for steady condition (as shown in Figure 7). The presented results in Figure 11 are when the flow amplitude is maximum (the peak of velocity amplitude during the first half of the cycle). With the increase of velocity, the vorticity increases for both cases since a higher fluid velocity creates vortices with higher rotationality, resulting in more intense vortices. However, it is noted that with the increase of velocity, more heat is brought out of the wake region behind the tube. Interestingly, it seems that the fluid that is flowing across the heat exchanger periodically leads to a wake region with better heat transfer performance.

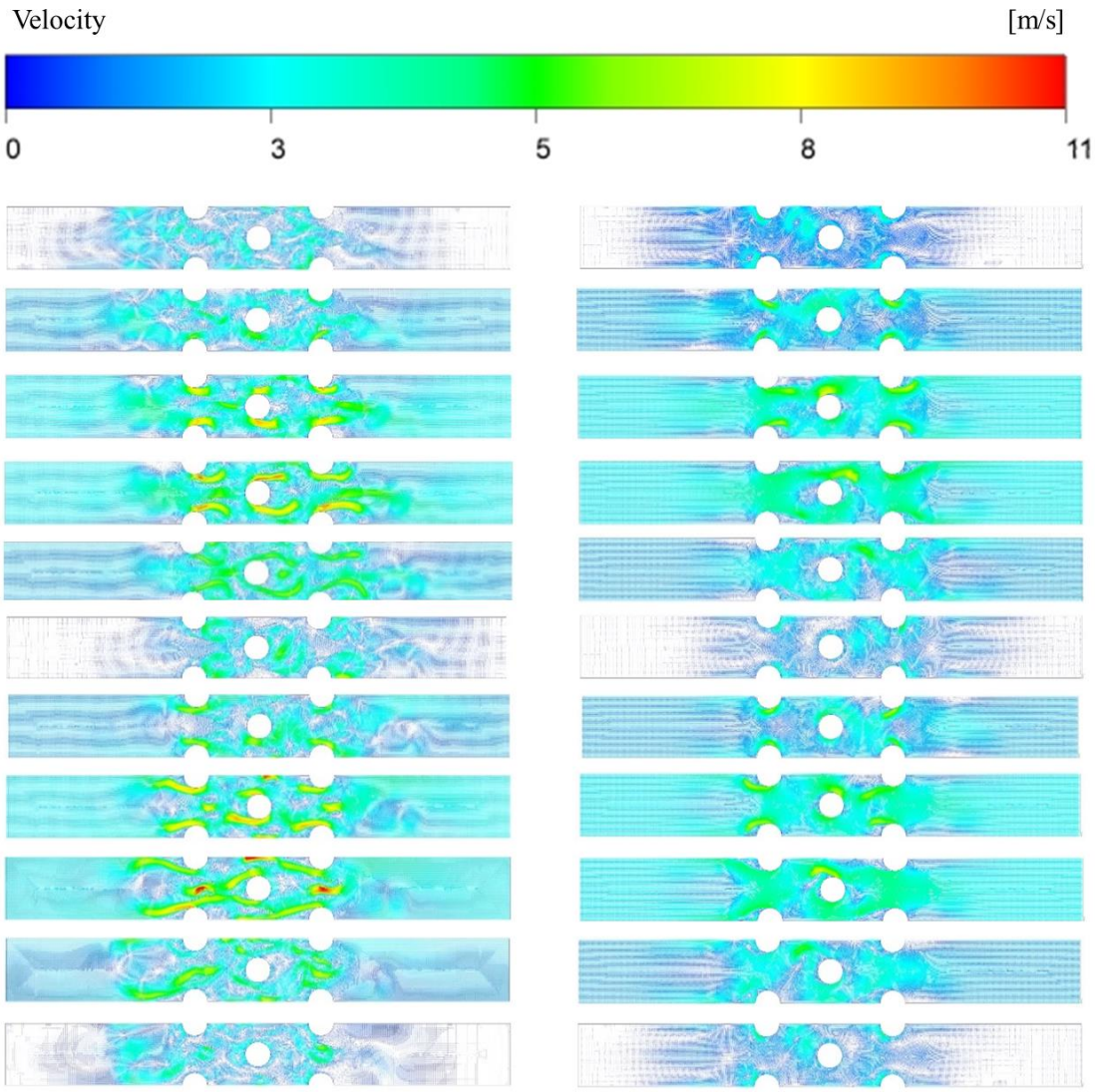

Fig. 10. Velocity vector within one flow cycle for oscillatory flow at a drive ratio of 1.2%

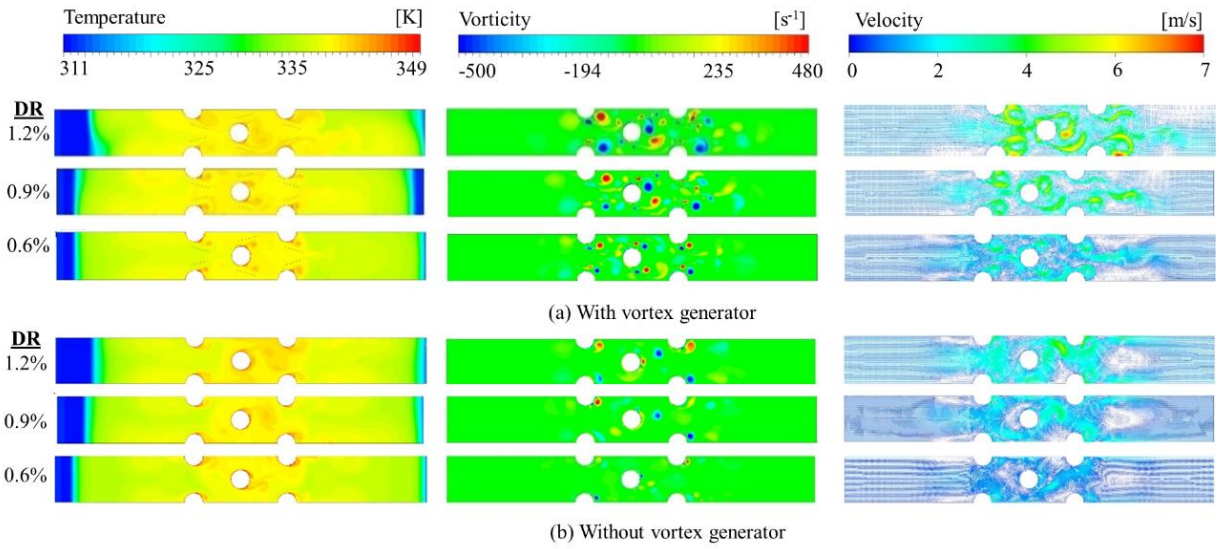

Fig. 11. Visualization of temperature contour (left), vortex contour (middle) and velocity vector plot (right) for cases with vortex and (without vortex at three different drive ratios of 1.2%, 0.9

Note that the presence of vortex generator increases the velocity along the vortex generator and tubes, creating higher vorticity. Also, comparison of velocity vector between cases with and without the vortex generator for drive ratio of 0.6% indicates that the wake region is reduced due to the presence of vortex generator. This reduction of wake region could be the reason for better heat transfer performance throughout the system which will be discussed in later section.

4.3 Comparison of Steady and Oscillatory Flow

Comparison is also done between the results from steady one-directional flow and the oscillatory flow conditions. Figure 12 shows visualisation plots of temperature, vorticity and velocity for both the steady case and the oscillatory flow cases. The results from oscillatory flow condition were taken when velocity of flow is at it's peak during the first half of the flow cycle. The temperature field within the area of tube banks is heated especially in the case of oscillatory flow. This is due to the cyclic nature of flow within the area and that heated fluid never really leave the system. In steady one-directional flow, the fluid flows over the tubes, pick up the heat and leaves. Hence, the temperature field remains low. For steady one directional flow, the inlet boundary temperature was set at 312 K however, at the outlet, the temperature of the fluid rises to 314 K. The fluid temperature that increases by 2 K proves the process of heat transfer between the tube banks and the fluid. However, in the case of oscillatory flow, both the left and right sides of the tube has a similar temperature throughout the oscillatory motion which is about 338K. Temperature values of flow in oscillatory motion are higher due to the fluid that is oscillating with time around the tubes and the heat is kept around the system whereas in steady case, the fluid brings the heat away and leaves the outlet.

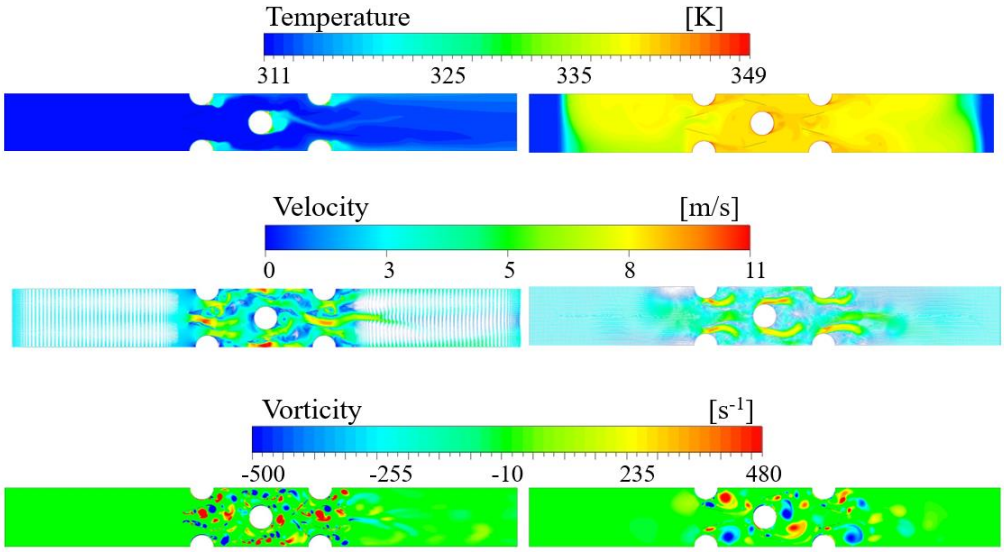

(a) Steady flow (2.55 m/s) (b) Oscillatory flow (2.65 m/s)

Fig. 12. Comparison of temperature contour (top), velocity vector (middle), and Vortici contour plot (bottom) for (a) steady and (b) oscillatory flow conditions

Velocity vector of the one-directional case shows that there are areas with low flow amplitude. However, these low flow amplitude areas are not clearly seen for oscillatory flow condition. This is probably due to the cyclic nature of flow that leads toward forward and backward movements of fluid across the structures hence pushing the stagnant area of flow away from the structure. This leads to a less rotationality in the oscillatory flow results (at least for this instantaneous plot for the peak of the cyclic flow). It is worth recalling that the oscillatory plot shown in Figure 12 is only

representing instantaneous result where the flow velocity is at maximum. As the fluid oscillates and changes it amplitudes during the flow cycle, rotationality of flow may change as well. This is the normal behaviour of the oscillatory flow condition. However, when the flow amplitude is at maximum, comparison between steady and oscillatory flow vortex pattern shows that the vorticity is more stable for the case of oscillatory flow condition.

Heat transfer data from three models of steady flow are then compared to the results of three models of oscillatory flow that has similar range of Reynolds Number with the steady cases. The Reynolds numbers of the oscillatory flow cases were calculated using the peak amplitude of velocity of the flow. Figure 13 shows the heat transfer results based on the plots of the Colburn-j factor, the final temperature, and the Colburn-j factor ratio. From Figure 13(a), the Colburn-j factor of the model for steady flow is shown to be higher compared to that for the oscillatory flow condition. The Colburn-j factor of the steady flow ranges from 0.013 to 0.022 while the Colburn-j factor for oscillatory flow ranges from 0.009 to 0.015. This could be related to the definition of temperature different in the calculation of the Colburn j-factor. This is as shown in Figure 13(b).

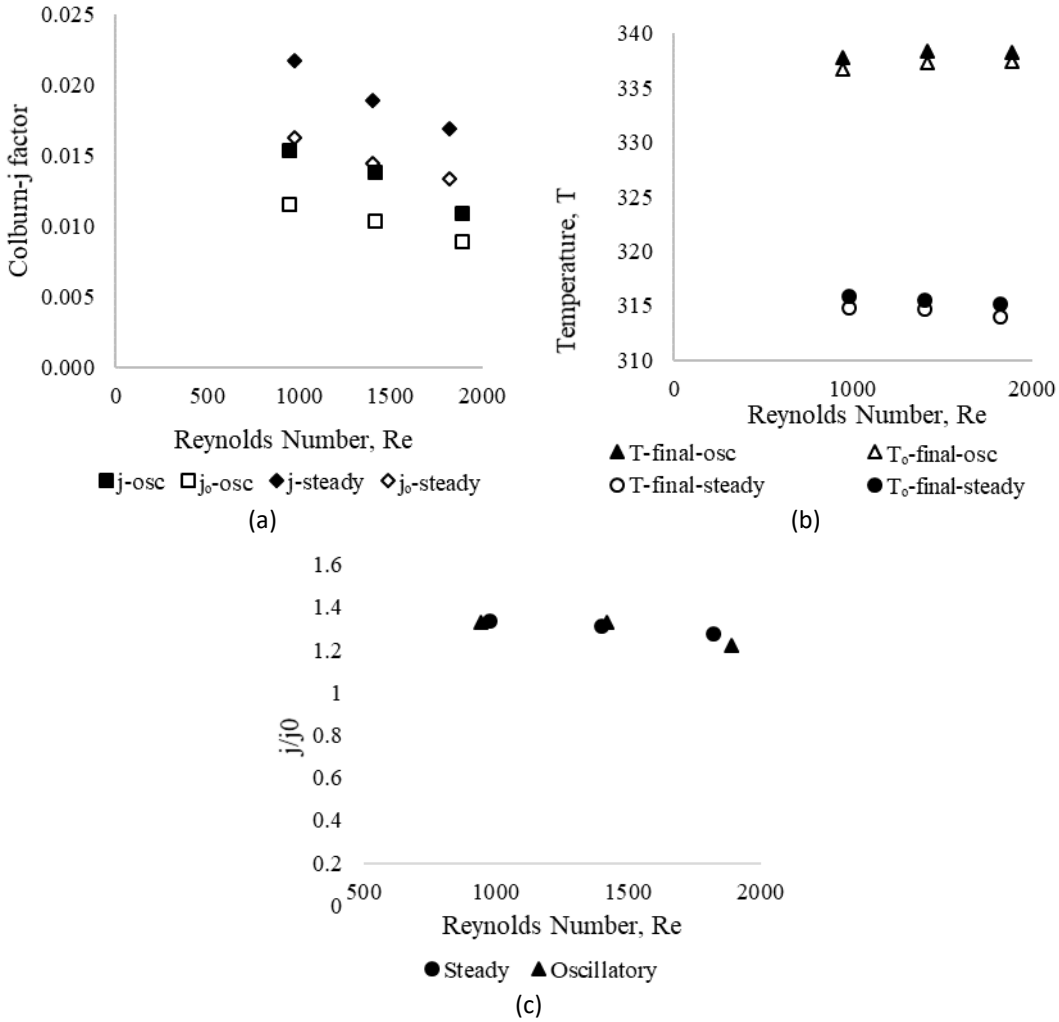

Fig. 13. Comparison of (a) Colburn-j factor, (b) final temperature, and (c) Colburn-j factor ratio between steady and oscillatory flow cases

It is observed that the final temperature of oscillatory flow ranges from 337K to 338K and they are relatively higher compared to the steady flow condition where temperature varies within the values of 314K and 316K. This is consistent with definition given in Eq. (8) to Eq. (10) where high

temperature leads to lower heat transfer coefficient and hence lower values of Nusselt and Colburn j-factor. However, when the results are plotted as the dimensionless form of the Colburn-j factor ratio similar results are seen for all the cases of steady and oscillatory flow cases. This is as shown in Figure 13 (c). Small differences of 0.28%, 1.39%, and 3.93% were recorded between the steady and oscillatory conditions for the three cases as the Reynolds number increases from 945 to 1891. A closer look at the non-dimensionless value of the Colburn j-factor yields that heat transfer in oscillatory flow is comparatively lower in amplitude compared to that of the steady flow condition, However, a higher final temperature of fluid is observed when oscillatory flow cases are compared to steady flow cases. This is consistent with the results in Figure 12. However, in term of dimensionless quantity, the performance of heat transfer enhancement for both the steady one-directional flow and the oscillatory flow conditions are similar, (i.e. Figure 13 (c)). Evidently, the low amplitude of heat transfer has been compensated by the high amplitude of fluids temperature if the calculation is done following this normal structure.

However, the research on heat transfer in oscillatory flow is not well established, hence it is unsure whether the use of the steady flow version of the Colburn-j factor correlation is accurate to represent the oscillatory flow condition. Steady flow heat transfer behaviour in this study varies from the heat transfer behaviour in the oscillatory flow condition. Hence, heat transfer correlations in steady flow might not be very suitable to be directly applied to the oscillatory flow cases. Further and careful analyses are required to define a better equation for oscillatory flow.

5. Conclusions

A two-dimensional (2D) computational fluid dynamics models of flow across tube banks with and without vortex generator were solved for steady one-directional and oscillatory flow conditions. It is found that a computational domain that cover wider area with more tubes in the direction of flow leads toward results that are closer to experimental values. The results show that the presence of vortex generator improves heat transfer in both steady and oscillatory flow, by an average of 21.46% and 29.45%, respectively. The steady flow models were validated with a published result, while the oscillatory flow models were verified with theoretical calculations. In the steady flow case, the temperature at the outlet slightly increases from the initial settings of inlet temperature. However, in the oscillatory case, since fluid oscillates and stay within certain travel distance inside the system, inlet and outlet conditions also change throughout the periodic motion. Both sides of inlet and outlet boundaries show rather similar values of high temperature, indicating a symmetrical condition between the first and second half of the oscillatory flow cycle. The comparison of heat transfer representation of Colburn j-factor for steady flow and oscillatory flow indicates that there is a need for a more detail analysis for heat transfer in oscillatory flow. Although the dimensionless values for both steady one-directional flow and the oscillatory flow are almost similar, the real amplitude of the non-dimensionless value is not. It is unclear whether the estimation of heat transfer in oscillatory flow using the steady one-directional equation is inaccurate. This calls for more investigations so that a better correlation can be found for heat transfer in oscillatory flow condition.

Acknowledgement

The authors would like to thank Universiti Teknikal Malaysia Melaka for supporting the research study. The research works are part of the works funded by Ministry of Higher Education Malaysia (RACER/2019/FKM-CaRE/F00407.

References

[1] Oneissi, Mohammad, Charbel Habchi, Serge Russeil, Daniel Bougeard, and Thierry Lemenand. "Novel design of delta winglet pair vortex generator for heat transfer enhancement." *International Journal of Thermal Sciences* 109 (2016): 1-9. https://doi.org/10.1016/j.ijthermalsci.2016.05.025

[2] Awais, Muhammad, and Arafat A. Bhuiyan. "Heat transfer enhancement using different types of vortex generators (VGs): A review on experimental and numerical activities." *Thermal Science and Engineering Progress* 5 (2018): 524-545. https://doi.org/10.1016/j.tsep.2018.02.007

[3] Awais, Muhammad, and Arafat A. Bhuiyan. "Enhancement of thermal and hydraulic performance of compact finned-tube heat exchanger using vortex generators (VGs): a parametric study." *International Journal of Thermal Sciences* 140 (2019): 154-166. https://doi.org/10.1016/j.ijthermalsci.2019.02.041

[4] Torii, Kwak, K. M. Kwak, and K. Nishino. "Heat transfer enhancement accompanying pressure-loss reduction with winglet-type vortex generators for fin-tube heat exchangers." *International Journal of Heat and Mass Transfer* 45, no. 18 (2002): 3795-3801. https://doi.org/10.1016/S0017-9310(02)00080-7

[5] Salviano, Leandro O., Daniel J. Dezan, and Jurandir I. Yanagihara. "Thermal-hydraulic performance optimization of inline and staggered fin-tube compact heat exchangers applying longitudinal vortex generators." *Applied Thermal Engineering* 95 (2016): 311-329. https://doi.org/10.1016/j.applthermaleng.2015.11.069

[6] Li, Hung-Yi, Wan-Rong Liao, Tian-Yang Li, and Yan-Zuo Chang. "Application of vortex generators to heat transfer enhancement of a pin-fin heat sink." *International Journal of Heat and Mass Transfer* 112 (2017): 940-949. https://doi.org/10.1016/j.ijheatmasstransfer.2017.05.032

[7] Zhai, C., M. D. Islam, R. Simmons, and I. Barsoum. "Heat transfer augmentation in a circular tube with delta winglet vortex generator pairs." *International Journal of Thermal Sciences* 140 (2019): 480-490. https://doi.org/10.1016/j.ijthermalsci.2019.03.020

[8] Song, KeWei, ZhiPeng Xi, Mei Su, LiangChen Wang, Xiang Wu, and LiangBi Wang. "Effect of geometric size of curved delta winglet vortex generators and tube pitch on heat transfer characteristics of fin-tube heat exchanger." *Experimental Thermal and Fluid Science* 82 (2017): 8-18. https://doi.org/10.1016/j.expthermflusci.2016.11.002

[9] Zdanski, P. S. B., D. Pauli, and F. A. L. Dauner. "Effects of delta winglet vortex generators on flow of air over in-line tube bank: A new empirical correlation for heat transfer prediction." *International Communications in Heat and Mass Transfer* 67 (2015): 89-96. https://doi.org/10.1016/j.icheatmasstransfer.2015.07.010

[10] Kamsanam, Wasan, Xiaoan Mao, and Artur J. Jaworski. "Development of experimental techniques for measurement of heat transfer rates in heat exchangers in oscillatory flows." *Experimental Thermal and Fluid Science* 62 (2015): 202-215. https://doi.org/10.1016/j.expthermflusci.2014.12.008

[11] Kamsanam, Wasan, Xiaoan Mao, and Artur J. Jaworski. "Thermal performance of finned-tube thermoacoustic heat exchangers in oscillatory flow conditions." *International Journal of Thermal Sciences* 101 (2016): 169-180. https://doi.org/10.1016/j.ijthermalsci.2015.10.032

[12] Jaworski, Artur J., and Antonio Piccolo. "Heat transfer processes in parallel-plate heat exchangers of thermoacoustic devices–numerical and experimental approaches." *Applied Thermal Engineering* 42 (2012): 145-153. https://doi.org/10.1016/j.applthermaleng.2012.03.014

[13] Ilori, Olusegun M., Artur J. Jaworski, and Xiaoan Mao. "Experimental and numerical investigations of thermal characteristics of heat exchangers in oscillatory flow." *Applied Thermal Engineering* 144 (2018): 910-925. https://doi.org/10.1016/j.applthermaleng.2018.07.073

[14] Rahman, Anas A., and Xiaoqing Zhang. "Prediction of oscillatory heat transfer coefficient for a thermoacoustic heat exchanger through artificial neural network technique." *International Journal of Heat and Mass Transfer* 124 (2018): 1088-1096. https://doi.org/10.1016/j.ijheatmasstransfer.2018.04.035

[15] Abd Elaziz, Mohamed, Ammar H. Elsheikh, and Swellam W. Sharshir. "Improved prediction of oscillatory heat transfer coefficient for a thermoacoustic heat exchanger using modified adaptive neuro-fuzzy inference system." *International Journal of Refrigeration* 102 (2019): 47-54.

https://doi.org/10.1016/j.ijrefrig.2019.03.009
[16] Chen, Geng, Yufan Wang, Lihua Tang, Kai Wang, and Zhibin Yu. "Large eddy simulation of thermally induced oscillatory flow in a thermoacoustic engine." *Applied Energy* 276 (2020): 115458. https://doi.org/10.1016/j.apenergy.2020.115458
[17] Feng, Ye, Ke Tang, Tao Jin, and Kaihao Zhang. "Impact of cross-sectional area ratio on time-averaged pressure drop induced by jet pump for thermoacoustic engine." *Energy Procedia* 142 (2017): 337-342. https://doi.org/10.1016/j.egypro.2017.12.053
[18] Rahpeima, R., and R. Ebrahimi. "Numerical investigation of the effect of stack geometrical parameters and thermo-physical properties on performance of a standing wave thermoacoustic refrigerator." *Applied Thermal Engineering* 149 (2019): 1203-1214. https://doi.org/10.1016/j.applthermaleng.2018.12.093
[19] Yahya, Samir Gh, Xiaoan Mao, and Artur J. Jaworski. "Experimental investigation of thermal performance of random stack materials for use in standing wave thermoacoustic refrigerators." *international journal of refrigeration* 75 (2017): 52-63. https://doi.org/10.1016/j.ijrefrig.2017.01.013
[20] Bhuiyan, Arafat A., M. Ruhul Amin, and AKM Sadrul Islam. "Three-dimensional performance analysis of plain fin tube heat exchangers in transitional regime." *Applied Thermal Engineering* 50, no. 1 (2013): 445-454. https://doi.org/10.1016/j.applthermaleng.2012.07.034
[21] Bhuiyan, Arafat A., M. Ruhul Amin, Rezwanul Karim, and A. K. M. S. Islam. "Plate fin and tube heat exchanger modeling: Effects of performance parameters for turbulent flow regime." *International Journal of Automotive and Mechanical Engineering* 9, no. 1 (2014): 1768-1781. https://doi.org/10.15282/ijame.9.2013.25.0147
[22] Alamir, Mahmoud A. "Thermoacoustic Energy Conversion Devices: Novel Insights." *Journal of Advanced Research in Fluid Mechanics and Thermal Sciences* 77, no. 2 (2021): 130-144. https://doi.org/10.37934/arfmts.77.2.130144
[23] Fatimah Al Zahrah Mohd Saat, Dahlia Johari, and Ernie Mattokit. "DeltaE Modelling and Experimental Study of a Standing Wave Thermoacoustic Test Rig." *Journal of Advanced Researched in Fluid Mechanics and Thermal Sciences* 60, no.2 (2019): 155-165.